DOI 10.1007/s11015-015-0098-1
*Metallurgist Vol. 59, Nos. 3–4, July, 2015 (Russian Original Nos. 3–4, March–April, 2015)*

# BEHAVIOR OF EXTRUSION BRIQUETTES (BREX) IN MIDREX REACTORS. PART 1

**A. M. Bizhanov,[1] I. F. Kurunov,[2] and A. Kh. Wakeel[1]**

UDC 669.162:669.181.24

*Results are presented from cage tests of the metallization of extrusion briquettes (brex) in an industrial Midrex reactor. The brex are made by the stiff vacuum extrusion of dispersed iron-bearing waste products with the use of different binder materials. The structures of the initial and metallized brex were studied on the basis of data obtained by optical and electron microscopy. The degree of metallization was 90.92–96.65% for brex made with the use of different binders in different amounts.*

***Keywords*:** *stiff vacuum extrusion, extrusion briquette (brex), strength, porosity, binder, Midrex reactor, metallization.*

Within recent years, the stiff vacuum extrusion of finely dispersed technogenic and natural metallurgical materials has gained recognition as a proven technology for making extrusion briquettes (brex) for refining furnaces (blast furnaces, ore-roasting furnaces, electric-arc steelmaking furnaces, etc.) [1–5]. This article examines results from experiments performed to assess the potential for the metallization of brex in reactors designed for the direct reduction of iron (DRI). The experiments were conducted in an industrial Midrex reactor operated by the company Qatar Steel (Qatar, Doha). Qatar Steel annually imports 3.5 million tons of iron-ore pellets to produce 2.35 million tons of hot-briquetted iron (HBI). Tens of thousands of tons of finely dispersed iron-bearing wastes are formed each year during the unloading, storage, and subsequent charging of pellets into metallization reactors, discharging of the metallized pellets, and their briquetting. To conduct the tests, we used brex produced from a mixture of pellet screenings – 55.6% (no more than 92% of which were 6.3 mm or smaller in size), metallized sludge – 27.8% (also having a 92% content of particles no coarser than 6.3 mm), and mill scale – 16.6% (99% no coarser than 10 mm). The main goals of the investigation were to evaluate the melting properties of brex in the Midrex process and to select a binder that would give the brex the necessary strength and maximize their metallization. The mixture was subjected to additional comminution (Fig. 1) on a roll crusher before it was briquetted. Table 1 shows the chemical composition of the components of the mixture.

Four types of experimental brex were tested (Table 2). The types differed negligibly from one another in their chemical composition and were distinguished only by the type of binder and the amount of binder that was used. The brex were made by the company J. C. Steele & Sons on a laboratory extruder. The mixture was prepared and homogenized by using a Hobart laboratory mixer that simulated the processing of the charge in a clay mill with a vacuum seal.

There was a substantial difference (Table 3) between the green brex and the brex after strengthening (after their aging for 14 days).

[1] J. C. Steele & Sons, Statesville, NC, U.S.; e-mail: abizhanov@jcsteele.com.
[2] Novolipetsk Metallurgical Combine, Lipetsk, Russia; e-mail: kurunov_if@nlmk.com.
[3] Qatar Steel Company, State Mesaieed, Qatar; e-mail: wakeel@qatarsteel.com.qa.

Translated from Metallurg, No. 4, pp. 16–20, April, 2015. Original article submitted March 20, 2015.

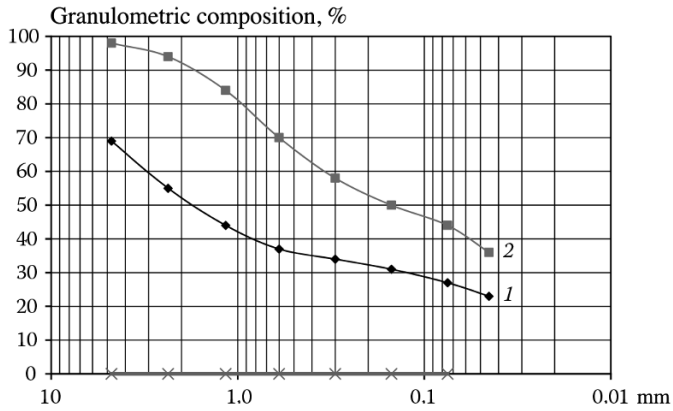


Fig. 1. Granulometric composition of the mixture of materials used at Qatar Steel for briquetting: *1*) initial mixture; *2*) after additional comminution (the maxima on the curves correspond to the mixture's content of particles smaller than 5 mm).

TABLE 1. Chemical Composition of the Components of the Mixture Used by the Company Qatar Steel to Make Brex

| Elements and oxides | Content in the component, wt.% | | |
|---|---|---|---|
| | pellet screenings | sludge | scale |
| Fe | 65.0 | 66.6 | 70.0 |
| $SiO_2$ + CaO | 3.8 | 6.52 | 1.00 |
| CaO | 1.3 | 4.38 | 0.15 |
| MgO | 0.75 | 0.69 | 0.10 |
| $Al_2O_3$ | 0.95 | 0.83 | 0.25 |
| MnO | 0.1 | 0.16 | 1.20 |
| P | 0.055 | 0.045 | 0.02 |
| $TiO_2$ | – | 0.010 | 0.020 |
| $V_2O_5$ | – | 0.12 | 0.025 |
| C | – | – | 0.30 |
| S | 0.015 | 0.01 | 0.015 |
| $Na_2O + K_2O$ | – | 0.33 | – |

TABLE 2. Component-by-Component Composition of the Brex

| Components of the charge | Type of briquette | | | |
|---|---|---|---|---|
| | 01–01 | 01–02 | 01–03 | 01–04 |
| Mixture of pellet screenings, sludge, and scale | 95.0 | 95.0 | 91.5 | 92.0 |
| Slaked lime | 5.0 | – | – | 6.0 |
| Portland cement | – | 5.0 | 8.0 | – |
| Bentonite | – | – | 0.5 | – |
| Molasses | – | – | – | 2.0 |

TABLE 3. Physico-Mechanical Properties of Brex after Aging

| Properties | Type of brex | | | |
|---|---|---|---|---|
| | 01–01 | 01–02 | 01–03 | 01–04 |
| Density,[1] g/cm$^3$ | 3.314 | 3.458 | 3.300 | 3.464 |
| Density,[2] g/cm$^3$ | 3.085 | 3.005 | 2.844 | 3.038 |
| Compressive strength[1], N/mm$^2$ | 2.2 | 1.6 | 1.6 | 18.4 |
| Moisture content,[1] % | 11.5 | 10.5 | 9.8 | 8.9 |
| Moisture content,[2] % | 1.11 | 1.07 | 1.06 | 2.53 |

[1] Green briquettes. [2] Strengthened briquettes.

TABLE 4. Morphological Parameters of the Pore Microstructure in Brex Specimens

| Type of briquette | Parameters | Class of pores | | | | | | $n_{im}$, % | $K_a$, % |
|---|---|---|---|---|---|---|---|---|---|
| | | $D_1$ (<0.1 μm) | $D_2$ (0.1–1.0 μm) | $D_3$ (1.0–10 μm) | $D_4$ (10–100 μm) | $D_5$ (>100 μm) | $D_{max}$, μm | | |
| 01–01 | $N$, % | 0.7 | 13.5 | 56.2 | 29.6 | – | 32.36 | 21.25 | 8.50 |
| | $K_f$ | 0.42–0.50; 0.58–0.67 | | | | | | | |
| 01–03 | $N$, % | 1.9 | 18.2 | 46.9 | 33.1 | – | 32.2 | 20.88 | 17.69 |
| | $K_f$ | 0.33–0.42; 0.50–0.58 | | | | | | | |

**Notes:** 1. $N$ represents pores of different size classes expressed as fractions of the total number of pores $n_{im}$ calculated from the SEM-image; $D_1$–$D_5$ are the different pore-size classes; $D_{max}$ is the maximum equivalent diameter of the pores; $K_a$ is the anisotropy coefficient, or the degree of orientation of the solid structural elements; $K_f$ is the shape factor of the pores. 2. The coefficient $K_f$ is calculated as the ratio of the semi-minor of an ellipse inscribed in a pore to its semi-major axis. The coefficient $K_f$ = 0.66–1.00 for isometric pores, $K_f$ = 0.1–0.66 for anisometric pores, and $K_f$ < 0.1 for slit-shaped pores.

The porosity of brex is one of their most important properties and determines their reducibility. The microstructure of the specimens and the specifics of their porosity were investigated with the use of scanning electron microscope (SEM) LEO 1450 VP (Carl Zeiss, Germany) with a guaranteed resolution of 3.5 nm and STIMAN software [6] to quantitatively analyze SEM images obtained in the reflected-electron regime. The porosity of briquette specimens 01–01 and 01–03 was studied on material that was freshly cleaved from the specimens' surface. Morphological studies of the microstructure were performed in the secondary-electron regime and allowed us obtain high-quality half-tone images over a broad range of magnifications. The STIMAN method makes it possible to obtain correct images with distinct boundaries between the pores and the particles. The thus-measured morphological parameters of brex 01–01 and 01–03 and the characteristics of the pores are shown in Table 4. This information clearly shows that the only significant difference in the porosity of the specimens was with respect to the anisotropy coefficient. This difference was probably due to the type of binder.

The distribution of the macropores (with sizes greater than 100 μm) can be determined by computer-assisted x-ray tomography. The images in Fig. 2 illustrate the difference in the distributions of the macropores in green brex specimens 01–01 and 01–03. The images were captured with a Yamato TDM-1000 x-ray computer microtomatograph (Japan). The magnification was 32 and the resolution was 11 μm. It can be concluded that the 01–01 brex had a higher percentage of pores larger than 100 μm than did the 01–03 brex.

The degree of open porosity determined by the STIMAN method is very consistent with the open porosity measured by liquid saturation in a vacuum in accordance with the standard DIN 51056 (GOST 26450.1–85). The porosity values were within the range 21–24% for the specimens that were examined.

We conducted two series of cage tests that entailed the reduction of brex in an industrial Midrex reactor. In the first series, from 25 to 30 strengthened brex were placed inside rigid steel cages (Fig. 3*a*) that were then charged into the reactor

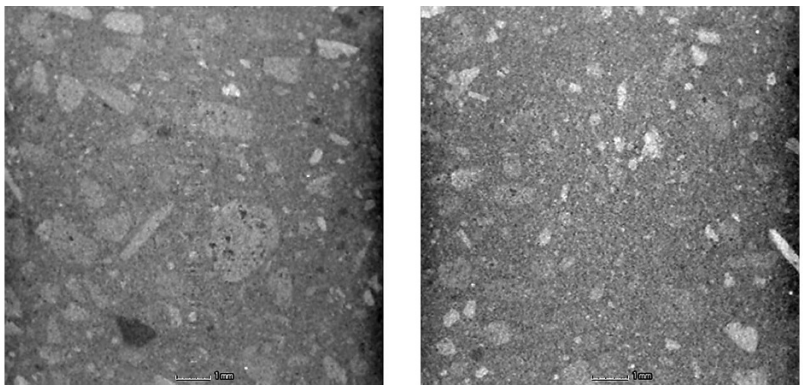

*a* *b*

Fig. 2. Distribution of pores coarser than 100 μm in specimens of briquettes 01–01 (*a*) and 01–03 (*b*) (micro-x-ray tomography).

*a* *b*

Fig. 3. Steel cages (*a*) and packets (*b*) for charging briquettes together with pellets into a Midrex reactor.

together with pellets. The brex were extricated from the reactor after the tests were concluded in order to be able to visually evaluate the condition of the reduced briquettes and study their composition and properties. The mechanical strength of the brex did not play a significant role in this case, since they were not subjected to the pressure of the column of charge materials. The stiffness of the cage completely prevented having the brex be subjected to pressure from the layer of pellets and thus possibly be deformed or fractured. In the second series of tests, brex were placed inside deformable gas-permeable steel packets (Fig. 3*b*), which made it possible to study their behavior under conditions similar to those encountered inside a layer of pellets in a Midrex reactor. The results of the first series of tests are discussed below.

Cracks could clearly be seen on brex specimens 01–02 and 01–03 after they were removed from the reactor (Fig. 4). Both specimens had been prepared with the use of a cement binder. There were more cracks in the specimens with the 01–03 designation, which had a higher binder content (see Table 2). It can be concluded that the hot strength of brex is related to their crushing strength. Brex specimens 01–02 and 01–03, which were weaker and less dense in the cold state (see Table 3), also had a lower hot strength. The lower value for hot strength was manifest in the formation of surface cracks in the brex, which is consistent with the results obtained from studying the hot strength of iron-ore pellets and comparing it to their crushing strength [7]. In the case of the pellets, there was also a negative dependence of hot strength on the ratio $Al_2O_3/SiO_2$. An increase in this ratio decreased the pellets' hot strength. Brex specimens 01–02 and 01–03, which exhibited a lower hot strength than brex prepared with a lime binder, had the highest value for elastic modulus due to the substantial amount of

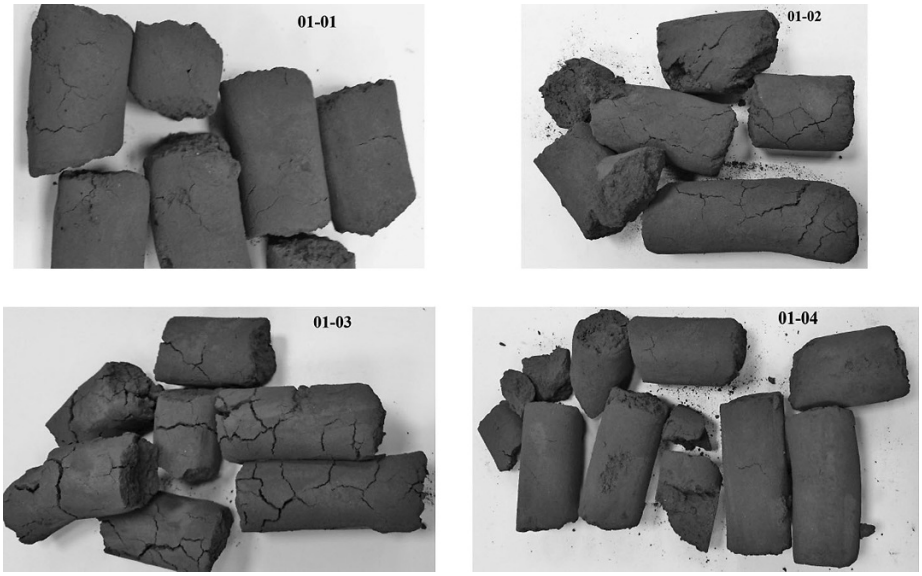


Fig. 4. Appearance of reduced briquettes after their removal from the rigid cages.

Fig. 5. Agglutination of 01–02 briquettes during solid-phase reduction.

alumina in the cement and, in particular, in the bentonite (brex 01–03). At the same time, the presence of lime and hematite (pellet screenings and scale) in brex 01–01 and 01–04 helped calcium ferrites form at just 400–500°C during the briquettes' heating in the Midrex reactor. These ferrites, which have low melting and softening points, strengthen the structure of brex and improve their reducibility [8].

Some of the brex with a cement binder became stuck to one another during their reduction (Fig. 5). The mechanism responsible for this is the same as the mechanism of agglutination of unfired pellets having a cement binder [9].

After the brex were extracted from the rigid steel cages, we determined their chemical composition, total iron content, content of metallic iron, and degree of metallization (Table 5). The highest degree of metallization was seen for the 01–01 brex with a 5% lime content, while the lowest degree of metallization was registered for the 01–03 brex with the maximal (8%) content of cement binder.

The changes in the porosity of the brex during their reduction were evaluated by using a Phoenix V|tome|XS 240 x-ray microtomatograph with two x-ray tubes: a microfocus tube with a maximum accelerating voltage of 240 kV and a power of 320 W; a nanofocus tube with a maximum accelerating voltage of 180 kV and a power of 15 W. The initial analysis

TABLE 5. Chemical Composition of the Green and Reduced Briquettes

| Type of briquette | Green briquette | | Reduced briquette | | | |
|---|---|---|---|---|---|---|
| | $Fe_t$ | C | $Fe_t$, % | $Fe_{met}$, % | Metallization, % | C, % |
| 01–01 | 64.53 | 2.32 | 80.07 | 77.39 | 96.65 | 0.984 |
| 01–02 | 64.06 | 1.88 | 79.22 | 74.63 | 94.21 | 0.836 |
| 01–03 | 62.53 | 1.72 | 75.2 | 68.37 | 90.92 | 0.874 |
| 01–04 | 60.46 | 2.6 | 76.4 | 70.17 | 91.85 | 1.7 |

TABLE 6. Volume and Number of Pores in Brex Specimens.

| Characteristics | Type of briquette (green/reduced) | |
|---|---|---|
| | 01–01 | 01–03 |
| Total volume of the pore space, $mm^3$ | 0.71666214/0.45010023 | 0.69426956/0.86682289 |
| Number of pores in the investigated volume of the specimen | 186063/93321 | 198420/241634 |

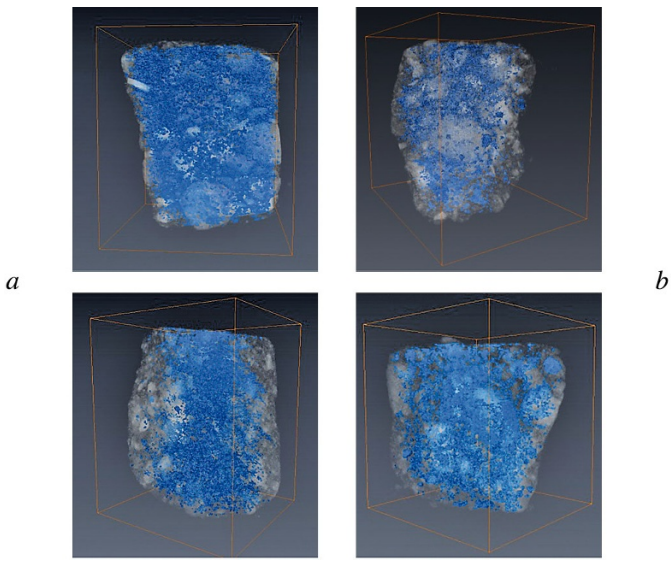

*a* *b*

Fig. 6. 3D-model of the pore space in a 01–01 briquette (*a*) and a 01–03 briquette (*b*).

of the data and the construction of a three-dimensional model of the specimens based on the x-ray photographs (projections) were done using the datoslx reconstruction software, while the software VGStudioMAX 2.1 and AvizoFire 7.1 were used to visualize and analyze the data based on elements of the three-dimensional image. The photographs were taken at an accelerating voltage of 100 kV and a current of 200 mA; the resolution during the recordings was 5.5 μm. Table 6 shows the results obtained from measuring the volume and number of pores in the brex before and after reduction. Figure 6 depicts the visualization of the pore distribution in the form of a 3D-model.

It is apparent that the porosity of the brex which were examined (and had coarse and ultra-coarse pores with a size of 1–100 μm or larger) changed in different directions. The total volume of the pore space decreased by a factor of 1.6 in the 01–01 brex and increased by 20% in the 01–03 brex. The increase in the porosity of the reduced brex having a cement binder

can be attributed to the disintegration of the cement stone at 850°C and the accompanying decrease in the strength of the brex. The brex remained intact thanks to the formation of a metallic matrix composed of reduced iron. Conversely, the reduction of the brex having a lime binder was accompanied by a decrease in their porosity. This can be attributed to the agglutination of fine pores during the formation of the metallic matrix composed of reduced iron.

**Conclusion.** Cage tests of brex made from a mixture of pellet screenings, mill scale, and finely dispersed wastes from HBI production in an industrial Midrex reactor showed that they can be effectively metallized without loss of integrity. The brex with a lime binder displayed the highest degree of metallization and the greatest strength. While the brex with a cement binder remained intact, cracks were formed on their surface. The number of cracks was found to be greatest in the brex with a higher binder content.

The authors thank Engineering Sciences Candidate, Professor T. V. Malysheva (Department of Extraction and Recycling, MISiS) and Engineering Sciences Candidate T. V. Nikitchenko (Development Director at the LGOK) for discussing the materials in the article and offering valuable comments.

## REFERENCES

1. I. F. Kurunov and A. M. Bizhanov, "Steele stiff vacuum extrusion – a promising method of agglomerating metallurgical raw materials and waste products," *Chern. Metall.: Byull. NTiEI*, No. 4, 46–49 (2012).
2. I. F. Kurunov, A. M. Bizhanov, D. N. Tikhonov, and N. R. Mansurova, "Metallurgical properties of briquettes," *Metallurg*, No. 6, 44–48 (2012).
3. I. F. Kurunov and A. M. Bizhanov, "Brex – a new stage in the agglomeration of raw materials for blast furnaces," *Metallurg*, No. 3, 49–53 (2014).
4. I. K. Dalmia, I. F. Kurunov, R. Stil, and A. M. Bizhanov, "Production of a new generation of briquettes and their use in blast-furnace smelting," *Metallurg*, No. 3, 39–41 (2112).
5. A. M. Bizhanov, G. S. Podgorodetskii, I. F. Kurunov, et al., "Extrusion briquettes (brex) for the production of ferroalloys," *Metallurg*, No. 2, 44–49 (2013).
6. V. N. Sokolov, D. I. Yurkovets, O. V. Razgulina, and V. N. Mel'nik, "Study of the microstructural characteristics of solids by the computer analysis of SEM-images," *Izv. RAN, Ser. Fizich.*, **68**, No. 9, 1332–1337 (2004).
7. S. Dwarapud and M. Ranjan, "Influence of oxide silicate melt phases on the RDI of iron ore pellets suitable for shaft furnace of direct reduction process," *ISIJ Int.*, **50**, No. 11, 1581–1589 (2010).
8. E. F. Vegman, B. N. Zherebin, A. N. Pokhvisnev, et al., *The Metallurgy of Iron: Textbook*, IKTs Akademkniga, Moscow (2004).